

The Role of Phosphoinositide 3-Kinase C2 α in Insulin Signaling^{*[S]}

Received for publication, May 29, 2007, and in revised form, July 13, 2007. Published, JBC Papers in Press, July 20, 2007, DOI 10.1074/jbc.M704357200

Marco Falasca^{†1,2}, William E. Hughes^{§3}, Veronica Dominguez^{†4}, Gianluca Sala^{†2}, Florentia Fostira^{†4}, Michelle Q. Fang^{§3}, Rosanna Cazzoli^{§3}, Peter R. Shepherd[¶], David E. James^{||3}, and Tania Maffucci^{†4}

From the [†]Inositide Signalling Group, Centre for Diabetes and Metabolic Medicine, Institute of Cell and Molecular Science, Barts and The London, Queen Mary's School of Medicine and Dentistry, University of London, 4 Newark Street, London E1 2AT, United Kingdom, the [§]Phospholipid Biology Group and the ^{||}Diabetes and Obesity Research Program, Garvan Institute of Medical Research, 384 Victoria Street, Sydney, New South Wales 2010, Australia, and the [¶]Department of Molecular Medicine and Pathology, Faculty of Medical and Health Sciences, University of Auckland, Auckland 1142, New Zealand

The members of the class II phosphoinositide 3-kinase (PI3K) family can be activated by several stimuli, indicating that these enzymes can regulate many intracellular processes. Nevertheless, to date, there has been no definitive identification of their *in vivo* product, their mechanism(s) of activation, or their precise intracellular roles. By metabolic labeling, we here identify phosphatidylinositol 3-phosphate as the sole *in vivo* product of the insulin-dependent activation of PI3K-C2 α , confirming the emerging role of such a phosphoinositide in signaling. We demonstrate that activation of PI3K-C2 α involves its recruitment to the plasma membrane and that activation is mediated by the GTPase TC10. This is the first report showing a membrane targeting-mediated mechanism of activation for PI3K-C2 α and that a small GTP-binding protein can activate a class II PI3K isoform. We also demonstrate that PI3K-C2 α contributes to maximal insulin-induced translocation of the glucose transporter GLUT4 to the plasma membrane and subsequent glucose uptake, definitely assessing the role of this enzyme in insulin signaling.

Phosphoinositide 3-kinases (PI3Ks)⁵ are a conserved family of lipid kinases that catalyze the phosphorylation of the 3'-position of the inositol ring of phosphoinositides. Their action leads to the generation of 3-phosphorylated phosphoinositides

at the plasma membrane or in specific cellular membrane compartments. Interaction between these lipids and distinct structural motifs such as pleckstrin homology and FYVE domains can regulate the activity of different proteins through their membrane targeting or direct modulation of their enzymatic activity. Not surprisingly then, PI3Ks play key roles in many physiological events, including cell proliferation and differentiation, apoptosis, cytoskeletal organization, and membrane trafficking (1, 2). Moreover, alterations in PI3K-dependent pathways are implicated in different diseases, including cancer and diabetes (3).

Eight mammalian PI3Ks have been identified, and they are now grouped into three classes according to their sequence homology and *in vitro* substrate specificity (4, 5). Class I PI3Ks are activated downstream of tyrosine kinases or G-protein-coupled receptors. Although *in vitro* they can phosphorylate phosphatidylinositol (PtdIns), PtdIns-4-P, and PtdIns-4,5-P₂, it is generally accepted that PtdIns-4,5-P₂ is their main substrate *in vivo*. The only member of the class III PI3K family is the human homolog of the yeast vesicular protein-sorting protein Vps34, a monomer that is generally considered to be responsible for generation of the constitutive pool of PtdIns-3-P in endosomes and to be involved in intracellular trafficking.

Class II PI3Ks were first identified by sequence homology to other PI3Ks (6–8). The three members of class II (PI3K-C2 α , PI3K-C2 β , and PI3K-C2 γ) are monomers of high molecular weight due to extensions at both the N and C termini. One feature of these enzymes is their insensitivity to PI3K inhibitors, with the α -isoform exhibiting high resistance to treatment with both wortmannin and LY294002 (9–11) and the β -isoform exhibiting resistance to LY294002 (12, 13). *In vitro* class II PI3Ks are able to catalyze the phosphorylation of both PtdIns and PtdIns-4-P, whereas they do not appear to phosphorylate PtdIns-4,5-P₂ (6–8). The main *in vivo* substrate of class II PI3Ks has remained elusive for a long time, and we proposed only recently that PtdIns-3-P might be the *in vivo* product of the class II enzyme PI3K-C2 β at least in the lysophosphatidic acid signaling cascade (13). A definitive identification of the *in vivo* products of class II PI3Ks is still missing.

Similarly, although several stimuli have been identified as being able to activate class II PI3Ks (8, 10, 14–18), only a few reports have actually revealed the physiological consequences of such activation and defined the precise intracellular role of

* This work was supported in part by Diabetes UK (RD Lawrence Fellowship BDA:RD04/0002884), British Heart Foundation Grant PG/06/022/20348 (to M. F.) and the Fondazione Carichieti. The costs of publication of this article were defrayed in part by the payment of page charges. This article must therefore be hereby marked "advertisement" in accordance with 18 U.S.C. Section 1734 solely to indicate this fact.

[S] The on-line version of this article (available at <http://www.jbc.org>) contains supplemental Figs. S1–S3.

¹ To whom correspondence should be addressed. Tel.: 44-20-7882-8243; Fax: 44-20-7882-2186; E-mail: m.falasca@qmul.ac.uk.

² Supported by Association for International Cancer Research Grant 05-127.

³ Supported by the National Health and Medical Research Council, Australia.

⁴ Supported by RD Lawrence Fellowship Grant BDA:RD04/0002884 from Diabetes UK.

⁵ The abbreviations used are: PI3Ks, phosphoinositide 3-kinases; PtdIns, phosphatidylinositol; GSVs, GLUT4 storage vesicles; HPLC, high pressure liquid chromatography; GSK-3 β , glycogen synthase kinase-3 β ; HA, hemagglutinin; shRNA, short hairpin RNA; EGFP, enhanced green fluorescent protein; GFP-2 \times FYVE^{Hrs}, green fluorescent protein-fused double FYVE domain from the hepatocyte growth factor-regulated tyrosine kinase substrate; TIRFM, total internal reflection fluorescence microscopy; PDGF, platelet-derived growth factor.

these enzymes (8). Examples include demonstration that PI3K-C2 β is required for migration of cancer cells (13) and cytoskeletal organization (19) and evidence that PI3K-C2 α is required for clathrin assembly (20), clathrin-mediated trafficking (16), ATP-dependent priming of neurosecretory granule exocytosis (21), and contraction of vascular smooth muscle cells (22). Much remains to be understood regarding the activation of the class II PI3Ks in other signaling pathways and their mechanism of activation. For example, it is known that insulin can activate PI3K-C2 α in adipocytes and muscle cells (10, 11), but the physiological consequences of such activation are still not defined. Similarly, the *in vivo* product of PI3K-C2 α in insulin signaling and its mechanism of regulation remain to be clarified.

Glucose disposal in skeletal muscle and adipose tissues, a critical event for the maintenance of glucose homeostasis within the body, requires the insulin-mediated translocation of the glucose transporter GLUT4 from intracellular storage sites to the plasma membrane (23, 24). GLUT4 translocation involves several steps, including reorganization of actin, formation of GLUT4 storage vesicles (GSVs), and movement of GSVs close to the plasma membrane. Once at the cell periphery, a regulated process of tethering, docking, and fusion of the vesicles allows the insertion of GLUT4 into the membrane and externalization, finally leading to glucose transport. With numerous molecules reported to be involved in this process, GLUT4 translocation/insertion/externalization is one of the most complicated and tightly regulated intracellular events, requiring a fine cross-talk between signaling and trafficking processes through mechanisms that are still poorly defined.

It is well established that GLUT4 translocation/externalization requires the activation of both a class I PI3K (25) and the small GTPase TC10 (26). The involvement of the class I PI3K target protein kinase B/Akt was proposed/demonstrated almost 10 years ago (27–30), but some Akt downstream effectors able to regulate GLUT4 translocation/externalization have been identified only recently (31, 32), and the potential Akt-dependent step in this process has been described (33). Similarly, there are still few examples of downstream effectors of TC10 activation (34–37). In this latter respect, we have demonstrated previously that insulin-mediated TC10 activation leads to generation of a pool of PtdIns-3-P at the plasma membrane of insulin-responsive cells (38), identifying this lipid as a downstream mediator of TC10 signals. We also reported that exogenous PtdIns-3-P is able to induce GLUT4 translocation (38), suggesting that the insulin/TC10-dependent pool of PtdIns-3-P could play a role in this process. The importance of PtdIns-3-P in glucose transport was subsequently confirmed by the observation that overexpression of myotubularin, a specific PtdIns-3-P phosphatase, impairs insulin-induced GLUT4 translocation (39). More recent data further suggested a critical role for PtdIns-3-P in GLUT4 translocation (40–42), although the role of the endogenously generated, insulin-dependent pool of PtdIns-3-P in GLUT4 translocation remains unclear.

By directly analyzing the phosphoinositides, we here identify PtdIns-3-P as the sole lipid product generated through PI3K-C2 α activation in the insulin signaling pathway. This is the first time that such analysis has been performed upon activation of a class II PI3K by *in vivo* metabolic labeling of cells and high

pressure liquid chromatography (HPLC). Our data also indicate that activation of PI3K-C2 α involves its insulin-dependent targeting to the lipid raft subdomains of the plasma membrane and is mediated by the small GTPase TC10. Finally, we demonstrate that PI3K-C2 α plays an important role in regulating GLUT4 translocation and glucose uptake, identifying, for the first time, the role of both this isoform and the endogenously generated, insulin-dependent pool of PtdIns-3-P in insulin signaling.

EXPERIMENTAL PROCEDURES

Materials—Anti-PI3K-C2 α antibody for confocal microscopy was a kind gift of Dr. Marcus Thelen (Institute for Research in Biomedicine, Bellinzona, Switzerland), and anti-PI3K-C2 α antibody for immunoprecipitation has been described (10). Anti-PI3K-C2 α antibody for Western blotting and anti-PI3K-C2 β and anti-flotillin antibodies were from BD Transduction Laboratories. Anti-p110 α (sc-7174), anti-p110 γ (sc-7177), anti-actin (sc-8432), and anti-Akt (sc-8312) antibodies were from Santa Cruz Biotechnology, Inc. Anti-phospho-Ser⁴⁷³ Akt, anti-phospho-Ser⁹ glycogen synthase kinase-3 β (GSK-3 β), and anti-GSK-3 β antibodies were from Cell Signaling Technology. Anti-hemagglutinin (HA) peptide antibody (16B12) was from Babco. Alexa 488-conjugated goat anti-mouse antibody and Alexa 594-conjugated wheat germ agglutinin were from Molecular Probes. Insulin was from Sigma, or alternatively, the human insulin analog ActrapidTM from Novo Nordisk was used.

Plasmids—Two distinct constructs were generated to specifically knock down PI3K-C2 α . First, the following oligomers, designed based on the sequence of rat PI3K-C2 α , were subcloned into a pSuper vector: PI3K-C2 α short hairpin RNA (shRNA), 5'-GATCCCCGTCCAGTACAGTGCAAAGTTCAAGAGACTTTGCACTGTGACTGGACTTTTTTGGAAA-3' (forward) and 5'-AGCTTTTCCAAAAAGTCCAGTACAGTGCAAAGTCTCTTGAACCTTTCAGTGTGACTGGACGGG-3' (reverse). The corresponding scrambled oligomers were 5'-GATCCCCGCCTTGAACACTGGACGATTCAGAGATTTCGTCCAGTGTTCAGGCTTTTTTGGAAA-3' (forward) and 5'-AGCTTTTCCAAAAAGCCTTGAACACTGGACGATCTCTTGAATTCGTCCAGTGTTCAGGCGGG-3' (reverse). Second, the following oligomers, designed based on the sequence of rat PI3K-C2 α , were subcloned into a pSuperior vector: 5'-GATCCCCGTACAGAATGAGGAGTGGTTCAAGAGACCACCTCCTCATTCTGTACTTTTTGGAAA-3' (forward) and 5'-AGTCTTTCCAAAAGTACAGAATGAGGAGTGGTCTCTTGAACCACCTCCTCATTCTGTACGGG-3' (reverse). Scrambled sequences in the pSuperior vector were also generated. TC10 mutant constructs were a kind gift of Dr. Jeffrey Pessin (Stony Brook University, Stony Brook, NY). HA-GLUT4 from pBABE-puro-HA-GLUT4 (43) was cloned into pBABE-hygro via restriction enzyme digestion with BamHI and SalI. Enhanced green fluorescent protein (EGFP)-GLUT4 has been described (44).

Cell Cultures and Transfection—L6 cells were maintained in Dulbecco's modified Eagle's medium containing 10% fetal bovine serum plus penicillin/streptomycin and glutamine. Transfection of the pSuper-based recombinant vectors was

PI3K-C2 α /PtdIns-3-P Pathway in Insulin Signaling

performed using Lipofectamine (Invitrogen) according to the manufacturer. Single clones were selected in medium supplemented with 1.5 μ g/ml puromycin. To generate pSuperior-scrambled shRNA and pSuperior-shRNA PI3K-C2 α , L6 cells were infected with retroviral stocks generated by transfection of pVSVG (Clontech), pGag-pol (Clontech), and pSuperior-based vectors into human embryonic kidney 293 cells. Mixed cell populations were selected in medium supplemented with 1.5 μ g/ml puromycin. Electroporation of EGFP-GLUT4 DNA was performed as described (45). Briefly, cells from a confluent 10-cm dish were washed twice with α -minimal essential medium containing 10% fetal calf serum and then resuspended in 600 μ l of cytomix (120 mM KCl, 0.15 mM CaCl₂, 10 mM K₂HPO₄/KH₂PO₄ (pH 7.6), 25 mM HEPES (pH 7.6), 2 mM EGTA (pH 7.6), 5 mM MgCl₂, 2 mM ATP, and 5 mM glutathione) before use. Cells were added to a 0.4-cm electroporation cuvette (Bio-Rad) containing 100 μ g of DNA, and electroporation was carried out at room temperature at 200 V, one pulse, and 10 ms with a BTX ECM 830 pulse generator. Cells were finally resuspended in α -minimal essential medium containing 10% fetal calf serum and plated in 2 \times 6-cm dishes.

HPLC Analysis—Cells plated in a 12-well plate were labeled with 15 μ Ci/well *myo*-[³H]inositol (PerkinElmer Life Sciences) in inositol-free medium M199 containing antibiotics and glutamine. After 24 h, cells were stimulated with 100 nM insulin, and phospholipids were extracted at different times of stimulation. After deacylation, samples were separated by HPLC on a PartiSphere 5- μ m strong anion exchange column (Whatman) using a nonlinear gradient of 1 mM EDTA (buffer A) and 1.3 M (NH₄)₂HPO₄ + 1 mM EDTA (pH 3.8) (buffer B) (0–1 min, 0% buffer B; 1–40 min, 0–5% buffer B; 40–41 min, 5–15% buffer B; 41–75 min, 15–24% buffer B; 75–76 min, 24–33% buffer B; 76–95 min, 33–60% buffer B; 95–96 min, 60–100% buffer B; 96–100 min, 100% buffer B; 100–101 min, 100 to 0% buffer B; and 101–121 min, 0% buffer B wash). The levels of glycerol-PtdIns-3-P in each sample were normalized to the levels of glycerol-PtdIns that were unaffected by insulin treatment or PI3K-C2 α knockdown. For the experiment shown in supplemental Fig. S2, parental L6 cells were plated in a 6-well plate and labeled with 30 μ Ci/well *myo*-[³H]inositol.

Confocal Microscopy Analysis—Microscopy was performed as described (38) using a Zeiss LSM 510 laser confocal microscope system connected to an Axiovert 100M microscope and a Zeiss 63 \times objective. Images were acquired and loaded using the TCS NT program (Version 1.6.587). No further processing of the images was done except for changes in brightness/contrast to better visualize the data. Images were collected at 3.5 μ m from the bottom, and all conditions were imaged at the same distance from the glass. Quantitative analysis of cells displaying localization of the green fluorescent protein-fused double FYVE domain from the hepatocyte growth factor-regulated tyrosine kinase substrate (GFP-2 \times FYVE^{Hrs}) to the plasma membrane was performed as described (38).

Subcellular Fractionation and Detergent-free Cell Fractionation—For subcellular fractionation, cells were scraped in 255 μ M sucrose, 20 mM HEPES, and 1 mM EDTA containing protease inhibitors and lysed by 12 passages with a 23-gauge nee-

dle. Crude plasma membranes were collected as a pellet after centrifugation at 20,000 \times g for 20 min at +4 $^{\circ}$ C. Supernatants were centrifuged at 40,000 \times g for 20 min at +4 $^{\circ}$ C to pellet the high density membranes. An additional centrifugation step of the corresponding supernatants (50,000 \times g, 75 min, +4 $^{\circ}$ C) separated the low density membranes from the cytosol. Separation of lipid raft fractions by detergent-free cell fractionation was performed as described (38).

PI3K-C2 α in Vitro Assay—PI3K-C2 α was immunoprecipitated from Myc- or Myc-TC10 mutant-transfected cells using a specific antibody, and *in vitro* assay was performed as described (10).

EGFP-GLUT4 Total Internal Reflection Fluorescence Microscopy (TIRFM) Analysis—EGFP-GLUT4-expressing cells were grown on 42-mm No. 1 glass coverslips and starved for 2 h in serum-free Dulbecco's modified Eagle's medium. Coverslips were gently washed with warm 0.5% bovine serum albumin in Krebs-Ringer/HEPES buffer (from a 10 \times Krebs-Ringer/HEPES stock of 1.36 M NaCl, 47 mM KCl, 12.5 mM MgSO₄ \cdot 7H₂O, 12 mM CaCl₂ \cdot 2H₂O, and 200 mM HEPES) and mounted in a prewarmed ROC chamber (PeCon, Erbach, Germany) with 1 ml of Krebs-Ringer/HEPES buffer in an insert P heated stage (PeCon) on a Axiovert 200M microscope fitted with an XL incubator (PeCon). Single isolated cells were identified and chosen with differential interference contrast and epifluorescence (excitation, 488/10 nm; and emission, 525/25 nm). For TIRFM imaging, cells were excited with the 488-nm line of a 100-milliwatt argon ion laser introduced at the appropriate incident angle through the TIRF slider and an alpha Plan-FLUAR 100 \times /1.45 oil objective and imaged (emission, 525/25 nm) using a Zeiss AxioCam MRm digital camera. Single or multiple (up to 20) cells were imaged every 0.5 min for 15 min; insulin (100 nM) was introduced (100 μ l of a 10 \times stock); and cells were imaged for an additional 30 min. Images were taken with an exposure time of 40 ms using \sim 12.5% maximal laser output. Under such conditions, no reduction in detected fluorescence through "bleaching" was observed (data not shown). Image stacks were background-subtracted using Image J software (rsb.info.nih.gov/ij/), and blinded, cells and regions of interest were chosen to exclude any excessive movement and increases in cell area seen after insulin stimulus. Approximately one-third of either scrambled or PI3K-C2 α knockdown cells from a single experiment were not further processed. Total fluorescence within the area of interest at each time point was normalized to the average total fluorescence of pre-stimulated cells (–5 to 0 min, f_0). Representative images were processed using Adobe Photoshop.

HA-GLUT4 Translocation and Glucose Uptake Assays—HA-GLUT4 translocation assay was performed as described (43). Glucose transport was determined by a method adapted from Ref. 46. Myoblasts in 6-well plates were serum-starved for 2 h and then incubated for 30 min in Krebs-Ringer/HEPES buffer containing 2% bovine serum albumin with or without 100 nM insulin. Glucose uptake was measured over 10 min in the presence of 40 μ M 2-deoxy[³H]glucose (0.5 μ Ci/well). Cells were washed with ice-cold phosphate-buffered saline and extracted with 1 ml of phosphate-buffered saline containing 0.05% SDS.

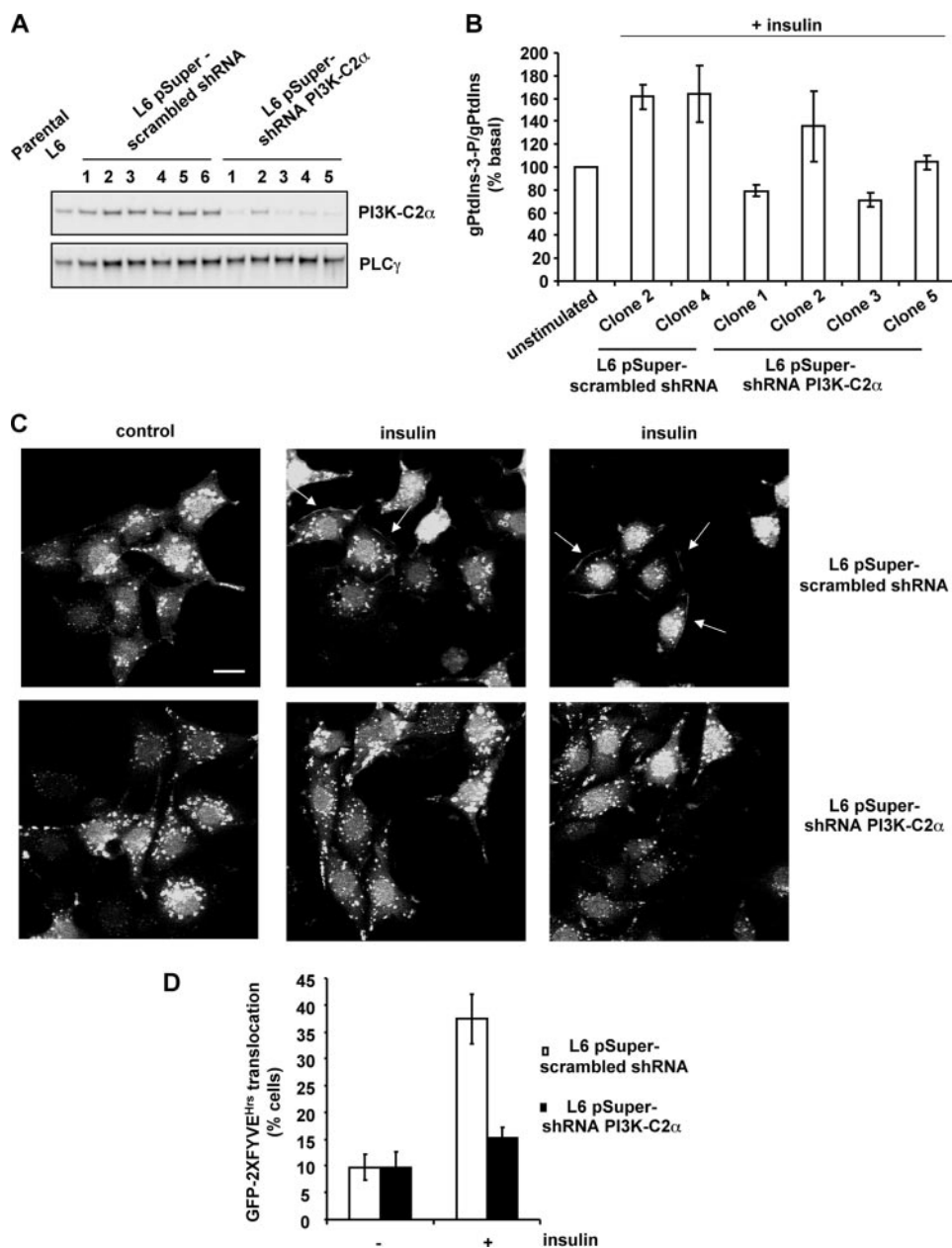


FIGURE 1. PI3K-C2 α specifically generates PtdIns-3-P upon insulin stimulation. Stable cell lines were generated by transfecting L6 cells with a control pSuper-scrambled shRNA or a specific pSuper-shRNA PI3K-C2 α vector. **A**, expression levels of PI3K-C2 α in the indicated clones compared with parental L6 cells. Equal loading was confirmed using anti-phospholipase C γ (PLC γ) antibody. **B**, HPLC analysis of the levels of PtdIns-3-P in 3 H-labeled scrambled cells (clones 2 and 4) and PI3K-C2 α knockdown cells (clones 1–3 and 5) upon 3 min of insulin stimulation. Data are means \pm S.E. from two to four independent experiments (scrambled, clones 2 ($n = 4$) and 4 ($n = 3$); and PI3K-C2 α knockdown, clones 1 ($n = 4$), 2 ($n = 2$), 3 ($n = 3$), and 5 ($n = 3$)). For each clone, the levels of PtdIns-3-P upon insulin stimulation are expressed as a percentage of the basal PtdIns-3-P levels in the same unstimulated clone. In these experiments, the absolute values of basal PtdIns-3-P were as follows: scrambled clones 2 (256.7 ± 47.5 cpm) and clone 4 (269 ± 175.5) and PI3K-C2 α knockdown clones 1 (367.2 ± 74.8 cpm), 2 (212.2 ± 49.7 cpm), 3 (252.2 ± 133.5 cpm), and 5 (176.2 ± 86.0 cpm). The difference between the basal levels of PtdIns-3-P in each of the PI3K-C2 α knockdown clones is not significant compared with the corresponding scrambled clone. *gPtdIns*, glycerol-PtdIns. **C**, confocal microscopy analysis of the indicated GFP-2 \times FYVE^{HIS}-expressing cells (scrambled clone 2 and PI3K-C2 α knockdown clone 1) left untreated or stimulated with insulin for 3 min. *Arrows* mark the plasma membrane localization. *Scale bar* = 10 μ m. **D**, quantitative analysis of experiments described for **C**. Data are means \pm S.E. from five independent experiments and are expressed as a percentage of cells displaying plasma membrane localization of GFP-2 \times FYVE^{HIS}.

was determined using 10 μ M cytochalasin B and subtracted from the total rates observed.

RESULTS

PI3K-C2 α Generates an Insulin-dependent Pool of PtdIns-3-P—We have reported previously that insulin generates a pool of PtdIns-3-P at the plasma membrane of muscle cells and adipocytes through activation of a PI3K more resistant to treatment with the inhibitors wortmannin and LY294002 (38). This observation, together with reports showing that PI3K-C2 α can be activated by insulin (10) and is very resistant to treatment with PI3K inhibitors (9–11), led us to hypothesize that such an isoform might catalyze the *de novo* synthesis of the insulin-mediated pool of PtdIns-3-P. To test this hypothesis, we generated L6 muscle cell lines stably knocked down for PI3K-C2 α using a recombinant pSuper vector containing the appropriate silencing shRNA. Control cells expressing the corresponding pSuper-scrambled shRNA were also generated. A significant reduction in the detectable protein levels was achieved in five different PI3K-C2 α knockdown clones, whereas no effect on PI3K-C2 α protein levels was observed in scrambled cells (Fig. 1A). No modulation of PI3K-C2 β (supplemental Fig. S1A) and the class I PI3K catalytic subunits p110 α and p110 γ (supplemental Fig. S1, B and C) was observed in the PI3K-C2 α knockdown cells. Furthermore, no difference in cell growth was detected between scrambled and PI3K-C2 α knockdown cells (supplemental Fig. S1, D and E).

To directly assess the effect of reduced PI3K-C2 α expression on the levels of the insulin-dependent pools of the 3-phosphorylated phosphoinositides, we performed metabolic labeling of the cells, followed by HPLC analysis. This technique represents the most accurate and

After incubation at 37 $^{\circ}$ C for 30 min, extracts were subjected to liquid scintillation counting. Protein determination was by bicinchoninic acid assay (Pierce). Nonspecific glucose uptake

direct way to analyze the levels of intracellular phosphoinositides. An example of the HPLC profile of parental L6 cells left untreated or stimulated with insulin is presented in supplement-

tal Fig. S2, specifically showing the insulin-induced increase in PtdIns-3-P levels, as reported previously (38). Scrambled and PI3K-C2 α knockdown clones were labeled with *myo*-[³H]inositol, and phosphoinositides from untreated and insulin-stimulated cells were extracted. HPLC analysis revealed that insulin increased the levels of PtdIns-3-P in two distinct scrambled clones (Fig. 1B). In contrast, knockdown of PI3K-C2 α completely inhibited the insulin-dependent generation of PtdIns-3-P (Fig. 1B) in three clones (clones 1, 3, and 5) expressing very low levels of PI3K-C2 α (Fig. 1A). Strikingly, insulin-mediated PtdIns-3-P synthesis was only slightly affected in one PI3K-C2 α knockdown cell line (clone 2) (Fig. 1B), consistent with the fact that this clone still retained appreciable levels of PI3K-C2 α expression (Fig. 1A). No difference in the basal levels of PtdIns-3-P was observed between scrambled and PI3K-C2 α knockdown cells (see the figure legend). Taken together, these data reveal that the levels of the insulin-dependent pool of PtdIns-3-P correlate with the levels of PI3K-C2 α expression and therefore demonstrate that PI3K-C2 α mediates the insulin-induced generation of PtdIns-3-P. To further assess the effect of PI3K-C2 α down-regulation on PtdIns-3-P generation, silenced and scrambled cells were transfected with the PtdIns-3-P-binding protein GFP-2 \times FYVE^{Hrs} (13, 38, 47). Confocal microscopy analysis revealed that GFP-2 \times FYVE^{Hrs} was localized exclusively in endosomal structures in resting cells, as described previously (13, 38, 47). A clear translocation of GFP-2 \times FYVE^{Hrs} to the plasma membrane was observed in scrambled cells upon insulin stimulation (Fig. 1C). These data indicated that, in these cells, the probe was able to detect the insulin-dependent pool of PtdIns-3-P generated at the cell surface, as already reported (38). No GFP-2 \times FYVE^{Hrs} translocation was observed in insulin-stimulated PI3K-C2 α knockdown cells (Fig. 1C). Quantitative analysis of these experiments revealed that there was no difference in the number of knockdown cells showing basal GFP-2 \times FYVE^{Hrs} staining at the plasma membrane compared with the scrambled cells (Fig. 1D). Upon insulin stimulation, a clear increase in the number of cells displaying plasma membrane localization of GFP-2 \times FYVE^{Hrs} was detected for scrambled but not knockdown cells (Fig. 1D), indicating that no PtdIns-3-P was generated at the plasma membrane of the knockdown cells upon insulin stimulation. Down-regulation of PI3K-C2 α did not appear to affect the endosomal localization of GFP-2 \times FYVE^{Hrs}, suggesting that PI3K-C2 α does not regulate the corresponding pool of PtdIns-3-P.

HPLC analysis also revealed that silencing PI3K-C2 α did not block the insulin-induced generation of PtdIns-3,4-P₂ and PtdIns-3,4,5-P₃ (data not shown), indicating that PI3K-C2 α is not required for the insulin-mediated synthesis of these two phosphoinositides. In addition, no difference in the platelet-derived growth factor (PDGF)-dependent generation of PtdIns-3,4-P₂ and PtdIns-3,4,5-P₃ was observed (data not shown), indicating that down-regulation of PI3K-C2 α does not affect other class I PI3K-dependent pathways. The levels of PtdIns-3-P did not change in PDGF-stimulated scrambled or PI3K-C2 α knockdown cells (data not shown), in agreement with our observation that PDGF does not generate PtdIns-3-P in L6 cells (38).

To further assess the specificity of the effect, we generated a second recombinant vector targeting a distinct sequence in PI3K-C2 α mRNA. L6 cells were retrovirally infected with such a vector (pSuperior-shRNA PI3K-C2 α) and a control pSuperior-scrambled shRNA, and the corresponding mixed populations were selected. No difference in cell growth was observed between the pSuperior-scrambled shRNA and pSuperior-shRNA PI3K-C2 α cells (data not shown). HPLC analysis revealed that the insulin-dependent generation of PtdIns-3-P was completely inhibited in pSuperior-shRNA PI3K-C2 α cells (supplemental Fig. S3A). The lack of PtdIns-3-P generation in these cells was not due to a reduced responsiveness to insulin because we detected a clear Akt phosphorylation as well as phosphorylation of its downstream target GSK-3 β in pSuperior-shRNA PI3K-C2 α cells at different times of insulin stimulation (supplemental Fig. S3B). Indeed, no effect on the insulin-induced synthesis of PtdIns-3,4,5-P₃ and PtdIns-3,4-P₂ was detected in pSuperior-shRNA PI3K-C2 α cells (supplemental Fig. S3, C–E), further indicating that PI3K-C2 α is not involved in the insulin-mediated synthesis of these phosphoinositides. These data indicate that the blockade of PtdIns-3-P production upon insulin stimulation is specifically associated with down-regulation of PI3K-C2 α . Taken together, these data demonstrate that PI3K-C2 α catalyzes specifically the *de novo* synthesis of an insulin-dependent pool of PtdIns-3-P at the plasma membrane. Because the insulin-dependent generation of PtdIns-3,4-P₂ or PtdIns-3,4,5-P₃ does not appear to be affected in PI3K-C2 α knockdown cells, these data identify, for the first time, PtdIns-3-P as the sole *in vivo* product of PI3K-C2 α , at least in the insulin signaling cascade.

PI3K-C2 α Translocates to the Plasma Membrane upon Insulin Stimulation—In an effort to better understand the mechanism of the insulin-mediated PI3K-C2 α regulation, we assessed whether activation of the enzyme is associated with an intracellular redistribution of the protein. Because PI3K-C2 α is localized intracellularly in resting cells (48, 49), whereas the *de novo* synthesis of PtdIns-3-P occurs at the plasma membrane (38), we hypothesized that insulin might relocate PI3K-C2 α to such a compartment. Confocal microscopy analyses revealed that endogenous PI3K-C2 α was localized in nuclei and the perinuclear region in resting cells (Fig. 2A), as reported previously (48, 49). Interestingly, insulin induced a rapid and transient translocation of endogenous PI3K-C2 α to the plasma membrane (Fig. 2A). Translocation was visible from 1.5 min after stimulation (Fig. 2A) and lasted \sim 10 min (data not shown). Similar data were obtained in subcellular fractionation studies (Fig. 2B). These data indicated that insulin not only activated PI3K-C2 α , but could also regulate the intracellular localization of this enzyme. More specifically, sucrose gradient fractionation indicated that insulin induced translocation of PI3K-C2 α to the lipid raft subdomain of the plasma membrane (Fig. 2C), a specialized compartment where the insulin-dependent pool of PtdIns-3-P is generated (38). These data suggest that the insulin-dependent, PI3K-C2 α -mediated generation of PtdIns-3-P at the plasma membrane requires the translocation of the enzyme in this compartment.

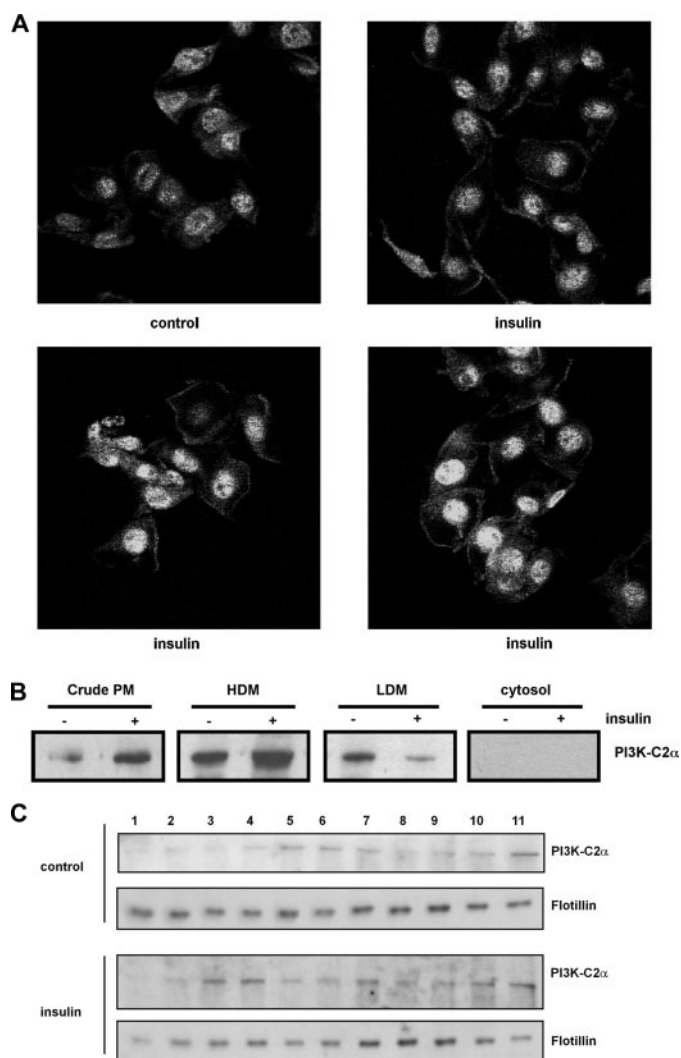


FIGURE 2. Insulin translocates PI3K-C2 α to the lipid raft subdomain of the plasma membrane. *A* and *B*, the intracellular localization of endogenous PI3K-C2 α in parental L6 cells left untreated or stimulated with 300 nM insulin for 1.5 min was assessed by confocal microscopy analysis and by subcellular fractionation, respectively. *PM*, plasma membrane; *HDM*, high density membrane; *LDM*, low density membrane. *C*, shown is the sucrose gradient fractionation of L6 cells left untreated or stimulated with 300 nM insulin for 1.5 min. The intracellular localization of PI3K-C2 α was determined using a specific antibody. Lipid raft fractions were identified using anti-flotillin antibody.

Insulin-mediated TC10 Activation Regulates PI3K-C2 α Activity—The small GTPase TC10 has been implicated in signaling required to generate the insulin-dependent pool of PtdIns-3-P (38). To establish whether PI3K-C2 α is specifically activated by TC10, L6 cells were transfected with a constitutively active or dominant-negative mutant of this protein, and activation of PI3K-C2 α was assessed by *in vitro* kinase assay. As shown in Fig. 3A, insulin activated PI3K-C2 α in mock-transfected L6 cells, as reported previously (10). Overexpression of the constitutively active TC10 mutant *per se* activated PI3K-C2 α to the same extent as insulin, whereas the dominant-negative TC10 mutant significantly inhibited the insulin-induced activation of the enzyme (Fig. 3A). Notably, we have reported that overexpression of the constitutively active TC10 mutant is sufficient to mimic the insulin-induced increase in PtdIns-3-P levels, whereas the dominant-negative TC10 mutant signifi-

cantly inhibits the insulin-induced formation of PtdIns-3-P (38). The observation that overexpression of these TC10 mutants resulted in similar effects on both PI3K-C2 α activation and PtdIns-3-P levels further indicates that PI3K-C2 α is responsible for the generation of the insulin-mediated, TC10-dependent PtdIns-3-P pool. Taken together, these data demonstrate that insulin activates PI3K-C2 α through the small GTPase TC10. This is the first report identifying an upstream mediator of insulin activation of PI3K-C2 α .

PI3K-C2 α Contributes to Maximal GLUT4 Translocation—Our observation that exogenous PtdIns-3-P is able to induce GLUT4 recruitment to the plasma membrane of L6 cells (38) suggests that this phosphoinositide is involved in this process. In addition, several lines of evidence indicate that one of the steps leading to complete GLUT4 translocation/externalization is insensitive to treatment with wortmannin (see “Discussion”), suggesting that wortmannin-resistant PI3K-C2 α may be involved. To check this hypothesis, we retrovirally infected L6 scrambled and PI3K-C2 α knockdown cells with HA-GLUT4 and performed a translocation assay enabling accurate assessment of the translocation of cellular HA-GLUT4 to the plasma membrane (43). Insulin clearly stimulated GLUT4 translocation in all scrambled clones tested (Fig. 4A). Translocation in scrambled and parental cells was comparable (data not shown), confirming that overexpression of the control vector does not affect the insulin-dependent response of the stable cell lines. In contrast, insulin-stimulated GLUT4 translocation was reduced in all PI3K-C2 α knockdown clones tested (Fig. 4A). The pooled data from all scrambled and all PI3K-C2 α knockdown clones are also shown (Fig. 4B).

Translocation was also assessed through single cell analysis of EGFP-GLUT4-expressing cells by TIRFM. No significant increase in EGFP fluorescence was detected at the cell surface of scrambled and PI3K-C2 α knockdown cells before treatment with insulin (–5 to 0 min) (Fig. 4C). After addition of insulin, an almost immediate relative increase in EGFP fluorescence was observed in all lines tested (within 10–12 s) (data not shown). A clear GLUT4 translocation was detected in two scrambled clones, whereas GLUT4 translocation was clearly inhibited in two PI3K-C2 α knockdown clones (Fig. 4C). Specifically, translocation was completely blocked in clone 1 (Fig. 4C), which had the most significant reduction in PI3K-C2 α levels (Fig. 1A) and a complete blockade of PtdIns-3-P production upon insulin stimulation (Fig. 1B). In contrast, clone 2 showed an intermediate but still significant reduction in insulin-induced GLUT4 translocation (Fig. 4C), consistent with the fact that such a clone retained appreciable levels of PI3K-C2 α (Fig. 1A) and insulin-induced PtdIns-3-P synthesis (Fig. 1B). Taken together, these data clearly indicate that PI3K-C2 α contributes to maximal insulin-induced GLUT4 translocation.

PI3K-C2 α Contributes to Maximal Glucose Uptake—We then investigated the effect of PI3K-C2 α knockdown on glucose uptake. In agreement with previous reports (50, 51), the insulin-induced glucose uptake in these cells was small but reproducible (Fig. 5, *A* and *B*). As for GLUT4 translocation, the insulin-induced glucose uptake in all scrambled clones and the parental cell lines was similar (data not shown). In contrast, the

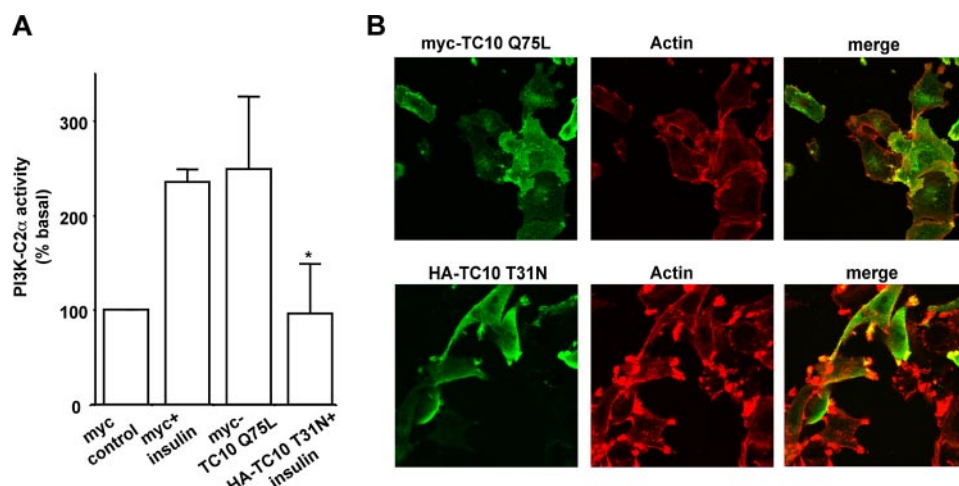


FIGURE 3. **Insulin activates PI3K-C2 α through TC10 activation.** *A*, serum-starved L6 cells expressing an empty vector (Myc), a constitutively active TC10 mutant (Myc-TC10 Q75L), or a dominant-negative TC10 mutant (HA-TC10 T31N) were left untreated or stimulated with 300 nM insulin for 2 min. PI3K-C2 α was immunoprecipitated, and activity was assessed by *in vitro* kinase assay. *, $p < 0.05$. *B*, the representative images are of transfected L6 cells showing the efficiency of transfection of the indicated constructs.

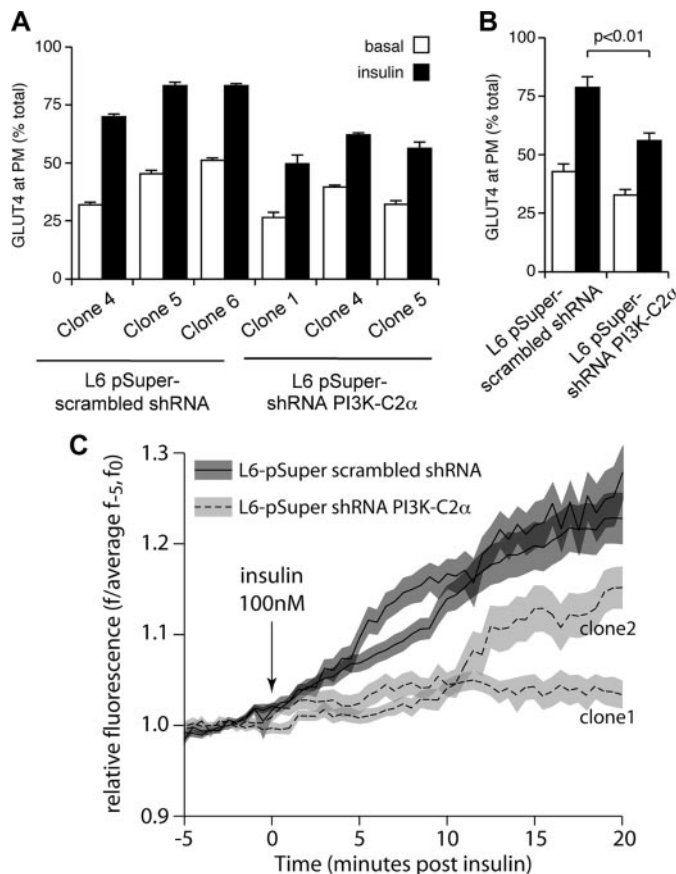


FIGURE 4. **PI3K-C2 α is required for maximal GLUT4 translocation.** *A*, GLUT4 translocation in the indicated clones stimulated with insulin for 20 min assessed as described under "Experimental Procedures." Data are means \pm S.E. from three independent experiments performed in the indicated scrambled and PI3K-C2 α knockdown clones. *PM*, plasma membrane. *B*, pooled data from all scrambled and all PI3K-C2 α knockdown clones ($p < 0.01$). *C*, TIRFM analysis of GLUT4 translocation in scrambled cells (clones 4 and 6; 37 and 38 cells, respectively, from six independent experiments) and PI3K-C2 α knockdown cells (clones 1 and 2; 18 cells from six independent experiments). At 5 min, the difference between PI3K-C2 α knockdown clone 1 and both scrambled clones was significant ($p < 0.001$). The difference between PI3K-C2 α knockdown clone 2 and the scrambled clones was significant at all time points (5 and 10 min, $p < 0.001$; and 15 and 20 min, $p < 0.05$).

insulin-stimulated response in the PI3K-C2 α knockdown clones was significantly reduced (Fig. 5, *A* and *B*), indicating that such an enzyme is involved in glucose uptake. These observations, together with our reported effect of exogenous PtdIns-3-P and wortmannin on GLUT4 translocation (38), strongly suggest that PI3K-C2 α contributes to maximal glucose uptake by generating an insulin-dependent pool of PtdIns-3-P able to direct GLUT4 to the plasma membrane.

It is noteworthy that both GLUT4 translocation and glucose uptake were inhibited in PI3K-C2 α knockdown cells despite a detectable insulin-dependent Akt phosphorylation at Ser⁴⁷³ (Fig. 5*C*) and GSK-3 β phosphorylation (Fig. 5*D*). The

insulin-induced Akt and GSK-3 β phosphorylation was detectable at all time points tested in the PI3K-C2 α knockdown cells (Fig. 5*D*). No difference in the PDGF-induced Akt phosphorylation was observed in PI3K-C2 α knockdown cells compared with scrambled cells (Fig. 5, *C* and *D*), further indicating that down-regulation of PI3K-C2 α does not affect other class I PI3K-dependent pathways.

DISCUSSION

PtdIns-3-P Is the Sole in Vivo Product of Insulin-stimulated Activation of PI3K-C2 α —During the last few years, it has become increasingly evident that pools of PtdIns-3-P can be specifically generated upon cellular stimulation (13, 38, 52–54), and PtdIns-3-P is emerging as a critical intracellular second messenger involved in different signaling pathways (54). Such renewed interest in PtdIns-3-P has inevitably led us to search for the enzyme(s) responsible for its generation. Sensitivity to PI3K inhibitors has suggested that some of these stimulated pools might be generated through activation of class II PI3K isoforms (13, 38).

Recently, interest in class II PI3Ks has progressively grown in parallel with the growing list of stimuli found to be able to activate them, including insulin (10), leptin and tumor necrosis factor- α (18), monocyte chemoattractant peptide-1 (14), and clathrin (16) in the case of PI3K-C2 α and insulin (17), platelet aggregation (15), and lysophosphatidic acid (13) in the case of PI3K-C2 β . Data also suggest that PI3K-C2 β is involved in epidermal growth factor- and stem cell factor-dependent signals (55). Despite all such evidence, much information about the class II PI3Ks is still missing (8). First, at the moment, there is no definitive identification of the *in vivo* product of class II PI3Ks. Evidence based on *in vitro* labeling of nuclear extracts suggests that PtdIns-3-P might be the product of a nuclear PI3K-C2 β (56, 57). Similarly, data obtained by indirectly analyzing PtdIns-3-P formation suggested that PI3K-C2 β might mediate the lysophosphatidic acid-dependent generation of PtdIns-3-P (13). More recently, HPLC analyses of [³H]inositol-labeled PC12

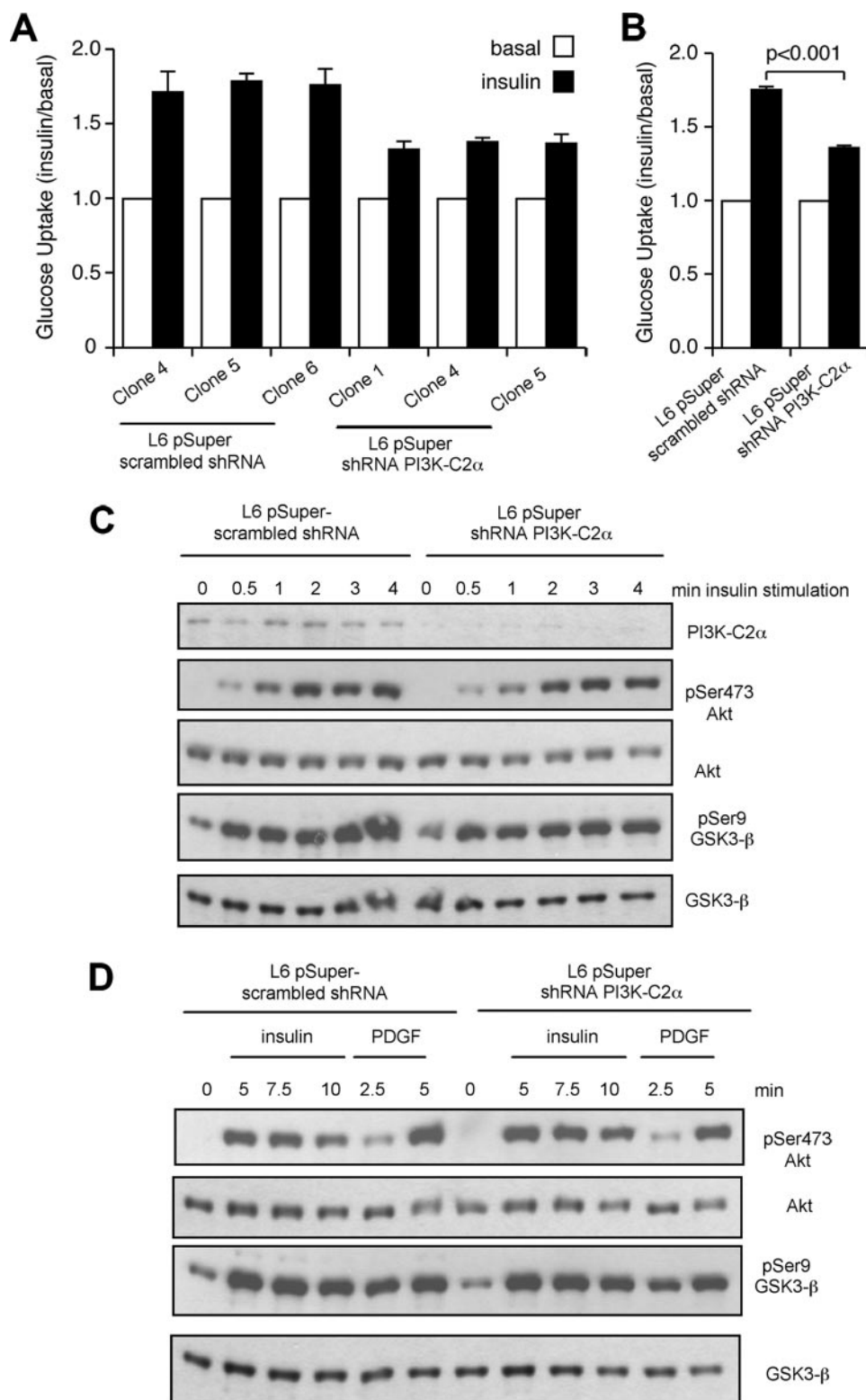


FIGURE 5. **PI3K-C2 α is required for maximal glucose uptake.** *A*, shown are the results from glucose transport assay in cells overexpressing HA-GLUT4. Data are from five independent experiments performed in the indicated scrambled and three PI3K-C2 α knockdown clones. For PI3K-C2 α knockdown clone 1, $p < 0.05$ versus scrambled clone 4, $p < 0.001$ versus scrambled clone 5, and $p < 0.01$ versus scrambled clone 6. For PI3K-C2 α knockdown clone 4, $p < 0.05$ versus scrambled clone 4, $p < 0.001$ versus scrambled clone 5, and $p = 0.01$ versus scrambled clone 6. For PI3K-C2 α knockdown clone 5, $p < 0.001$ versus scrambled clone 4, $p = 0.001$ versus scrambled clone 5, and $p < 0.05$ versus scrambled clone 6. *B*, shown are the pooled data from all scrambled and all PI3K-C2 α knockdown clones ($p < 0.001$). *C–D*, scrambled (clone 2) and PI3K-C2 α knockdown (clone 1) cells were stimulated with insulin or PDGF for the indicated times, and phosphorylation of Akt and GSK-3 β at Ser⁴⁷³ and Ser⁹, respectively, was assessed using specific antibodies. Membranes were stripped and reprobed with anti-Akt and anti-GSK-3 β antibodies.

cells revealed that overexpression of an inactive PI3K-C2 α mutant reduces the steady-state levels of both PtdIns-3-P and PtdIns-3,4,5-P₃ (21), but the effect of cellular stimulation of the enzyme was not assessed. Therefore, a clear analysis of the phosphoinositides generated downstream of class II PI3K activation obtained by *in vivo* labeling has yet to be performed. Second, although evidence suggests that activation of PI3K-C2 β might require proteolysis of the enzyme (12, 56, 57), a clear mechanism of activation of the different class II PI3Ks is still not defined. Third, only a few studies have actually defined the precise intracellular role of these enzymes (see the Introduction).

Our data provide the missing information about the function and regulation of the class II enzyme PI3K-C2 α in insulin signaling. First, HPLC analysis revealed that PtdIns-3-P is the only phosphoinositide generated through insulin-dependent PI3K-C2 α activation. PI3K-C2 α is not involved in generation of the insulin-dependent pools of PtdIns-3,4-P₂ and PtdIns-3,4,5-P₃. As far as we know, this is the first analysis of the different phosphoinositides generated downstream of activation of a class II PI3K enzyme performed by *in vivo* metabolic labeling of cells and HPLC analysis. These data (analyzing directly the phosphoinositides) identify, for the first time, PtdIns-3-P as the sole *in vivo* lipid product of the insulin-dependent activation of PI3K-C2 α . Data obtained using the probe GFP-2 \times FYVE^{Hrs} confirmed that PI3K-C2 α regulates the insulin-dependent pool of PtdIns-3-P at the plasma membrane. By identifying the enzyme responsible for its generation and a precise intracellular pathway regulating it, these data strongly support the emerging role of PtdIns-3-P as a novel dynamic intracellular second messenger (54).

Second, we have reported that PI3K-C2 α translocates to the lipid raft subdomain of the plasma membrane upon insulin stimulation, consistent with our demonstration

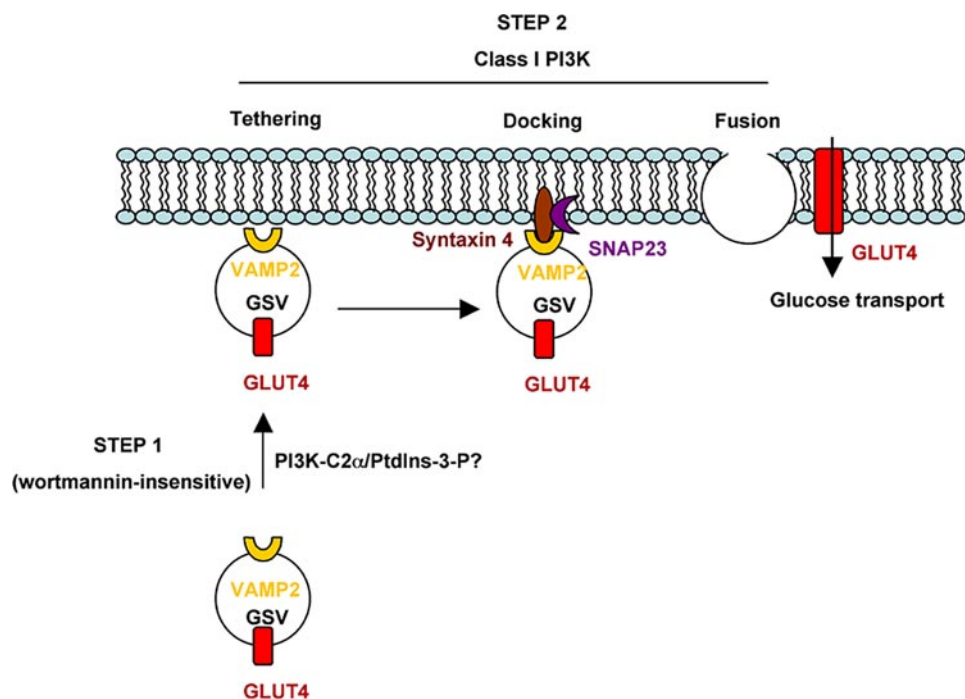


FIGURE 6. Schematic representation of GLUT4 translocation. GLUT4 translocation involves formation of GSVs and their movement to the cell periphery (step 1). Once close to the plasma membrane, GSVs need to be tethered and docked (primarily through an interaction between VAMP2 on GSVs and syntaxin-4/SNAP23 at the plasma membrane) to fuse with such a compartment (step 2). When GLUT4 is correctly inserted into the plasma membrane and partly externalized, it can mediate glucose transport. Evidence suggests that PI3K-C2 α and PtdIns-3-P might be involved in step 1 (see "Discussion"). On the other hand, data indicate that class I PI3K is not involved in step 1, whereas it is necessary for step 2. This representation is a simplified model of the process that actually involves several different proteins and different intermediate steps, including actin polymerization; GSV formation; and trafficking between the *trans*-Golgi network, endosomes, and GSVs.

that the *de novo* synthesis of PtdIns-3-P occurs in such a compartment (38). Relocation of PI3K-C2 α in such a specialized compartment is critical for activation of the enzyme. This is the first time that a membrane targeting-mediated mechanism of activation has been reported for PI3K-C2 α . These data, together with our previous observation that lysophosphatidic acid induces translocation of overexpressed PI3K-C2 β to the cell surface (13), suggest that recruitment to the membrane might represent a general mechanism of activation for class II PI3Ks. Moreover, our data clearly demonstrate that the insulin-dependent activation of PI3K-C2 α is mediated by the small GTPase TC10, in agreement with the role of this protein in insulin-induced PtdIns-3-P generation (38). Although there are data questioning the role of TC10 in insulin signaling (58, 59), more recent evidence shows that knockdown of TC10 α inhibits both GLUT4 translocation and glucose uptake (60), confirming the role of such a GTPase in insulin signaling. In this respect, it is important to emphasize that most of the previous reports actually suggested that some of the proteins proposed to be necessary for TC10 activation are not required for insulin signals (59), but they did not investigate the role of TC10 itself. Therefore, even taking into account such evidence, there is still the possibility that TC10 can be activated through a different mechanism. This is supported by the observation that overexpressed TC10 is activated by insulin in L6 myoblasts (38, 58) even in the absence of Cbl-associated protein expression and Cbl phosphorylation (58). Alternatively, we cannot rule out the possibility that the overexpressed TC10 mutant proteins used

in this study are mimicking the action of a different endogenous small GTPase.

Nevertheless, our data suggest that TC10 is required for the insulin-dependent activation of PI3K-C2 α , and they represent the first identification of an upstream mediator of the insulin-dependent activation of PI3K-C2 α . Furthermore, to our knowledge, this is the first report showing that a small GTPase can activate a class II PI3K isoform. In this respect, this work opens up new fields of investigation about the intriguing possibility that GTP-binding proteins can regulate class II PI3K activation.

The PI3K-C2 α -dependent Pool of PtdIns-3-P Is Necessary for Maximal GLUT4 Translocation and Glucose Uptake—The last unanswered question about PI3K-C2 α and insulin signaling concerned its role and function in such a pathway. Accumulating evidence suggests that PtdIns-3-P plays an important role in GLUT4 translocation (38–42).

GLUT4 translocation/externalization is a complex process, likely requiring tight cooperation between different pathways. Indeed, it has been shown that activation of a class I PI3K, which is necessary for the whole process to occur (25), is not sufficient to fully activate it (61–63). Similarly, although Akt is a key player in GLUT4 translocation (27–32), inhibition of its activity either by a specific chemical compound (33) or by gene silencing (33, 64) does not completely inhibit GLUT4 translocation, indicating that other, Akt-independent signals are also required. On the other hand, although data have revealed an important role for the GTPase TC10 in insulin signaling (26), knockdown of TC10 α only partially inhibits GLUT4 translocation and uptake (60), further supporting the hypothesis of a concerted activation of different pathways needed to properly activate glucose transport.

Although many intermediate steps have been described, recent data suggest that the whole process known as "GLUT4 translocation" might be broken down into two different and discrete steps: movement of GSVs to the cell periphery, *i.e.* close to the plasma membrane (step 1), and then their tethering, docking, and fusion with such a compartment (together referred here as step 2) (24, 41, 65, 66). Once correctly inserted into the plasma membrane and partly externalized, GLUT4 can mediate glucose transport. A simplified model of GLUT4 translocation is depicted in Fig. 6.

Notably, movement of the GSVs to the membrane is not inhibited by the PI3K inhibitors wortmannin (38, 41) and LY294002 (67) and does not appear to involve Akt activation (65), indicating that relocation of GSVs to the plasma mem-

brane (step 1) does not require activation of the class I PI3K pathway but rather involves motor proteins and microtubules (68, 69) and cytoskeletal rearrangement, possibly through TC10 activation (26). On the contrary, PI3K inhibitors block GLUT4 externalization (41, 67), indicating that class I PI3K activation is strictly necessary in the second step (Fig. 6). In this respect, recent evidence suggests that Akt might be the PI3K target necessary for tethering and docking of GSVs (33), whereas protein kinase C ζ and Munc18c (41, 70) might be the PI3K targets involved in fusion. A critical role for Akt in fusion has also been proposed (66), indicating that work still needs to be done to precisely define the PI3K-dependent players in the different steps. Furthermore, data have also suggested a role for TC10-dependent effectors in some of the step 2-associated processes (37), further supporting the hypothesis of a concerted action of the two pathways or even a cross-talk between them.

Here, we have shown that down-regulation of PI3K-C2 α inhibits GLUT4 translocation and glucose uptake even in the presence of a detectable insulin-dependent activation of Akt and GSK-3 β . It should be noted that inhibition of GLUT4 translocation in PI3K-C2 α knockdown cells was total or partial depending on the assays performed, and this is likely due to the different experimental conditions of the assays performed. Nevertheless, the key point is that all our data consistently demonstrate that knockdown of PI3K-C2 α impairs insulin-induced GLUT4 translocation and glucose uptake. The observation that knockdown of PI3K-C2 α resulted in only partial inhibition of glucose uptake but complete inhibition of insulin-induced PtdIns-3-P synthesis is consistent with the reported partial effect of TC10 α knockdown on glucose uptake (60) and with the hypothesis of different pathways required to fully activate glucose uptake.

These data, together with our previous observations (38), indicate that activation of a PI3K-C2 α /PtdIns-3-P pathway is required in some step(s) leading to GLUT4 translocation and glucose uptake. The precise mechanism of action of the PI3K-C2 α /PtdIns-3-P pathway, the intracellular effectors of PtdIns-3-P, and the precise step(s) of GLUT4 translocation involving PtdIns-3-P remain to be addressed. On the basis of the wortmannin insensitivity and our observation that exogenous PtdIns-3-P is able to move GLUT4 to the cell periphery but is not sufficient to induce glucose uptake (38), it is tempting to speculate that PI3K-C2 α /PtdIns-3-P might be involved in step 1 in the GLUT4 route to the plasma membrane (Fig. 6). This would be consistent with data suggesting a role for the TC10-dependent pathway in this step (26, 34) and with the hypothesis that PtdIns-3-P is important for translocation and possibly unmasking of the C-terminal domain of GLUT4 but not insertion into the plasma membrane (40). Other evidence suggests that PtdIns-3-P might be sufficient to induce both translocation and insertion into the membrane in the absence of Munc18c (41) or in 3T3-L1 adipocytes overexpressing 72-kDa inositol-polyphosphate 5-phosphatase (42). We cannot rule out the possibility that PI3K-C2 α /PtdIns-3-P might also play a role in some processes of step 2, acting in parallel with class I PI3K. In this respect, it is noteworthy that PI3K-C2 α is necessary for priming neurosecretory granule exocytosis (21) and that a role

for TC10 in exocytic vesicle fusion has been proposed recently (71).

In summary, this work defines, for the first time, the role of both PI3K-C2 α and the endogenously generated, insulin-dependent PtdIns-3-P pool in insulin signaling. Our data, together with all previous evidence, suggest that a parallel activation of a class I PI3K and PI3K-C2 α might be required for proper GLUT4 translocation and glucose uptake. Glucose transport appears to fail in insulin resistance accompanying several forms of diabetes. There is therefore a huge interest in understanding the alterations in signaling ultimately leading to such impairment. In this respect, the identification of PI3K-C2 α as a novel crucial player in insulin action would definitively prove useful in understanding the molecular mechanisms underlying insulin resistance to develop approaches to prevent type 2 diabetes.

Acknowledgments—We thank Dr. M. Thelen for the anti-PI3K-C2 α antibody; Dr. J. Pessin for the TC10 constructs; Dr. F. Cooke for help with HPLC experiments; C. Hohnen-Behrens, J. Davey, and D. Blair for help implementing the GLUT4 translocation assays; and L. Montuno (Carl Zeiss Australasia) for assistance with TIRFM.

REFERENCES

- Rameh, L. E., and Cantley, L. C. (1999) *J. Biol. Chem.* **274**, 8347–8350
- Cantley, L. C. (2002) *Science* **296**, 1655–1657
- Katso, R., Okkenhaug, K., Ahmadi, K., White, S., Timms, J., and Waterfield, M. D. (2001) *Annu. Rev. Cell Dev. Biol.* **17**, 615–675
- Vanhaesebroeck, B., Leeyers, S. J., Ahmadi, K., Timms, J., Katso, R., Driscoll, P. C., Woscholski, R., Parker, P. J., and Waterfield, M. D. (2001) *Annu. Rev. Biochem.* **70**, 535–602
- Foster, F. M., Traer, C. J., Abraham, S. M., and Fry, M. J. (2003) *J. Cell Sci.* **116**, 3037–3040
- MacDougall, L. K., Domin, J., and Waterfield, M. D. (1995) *Curr. Biol.* **5**, 1404–1415
- Virbasius, J. V., Guilherme, A., and Czech, M. P. (1996) *J. Biol. Chem.* **271**, 13304–13307
- Falasca, M., and Maffucci, T. (2007) *Biochem. Soc. Trans.* **35**, 211–214
- Domin, J., Pages, F., Volinia, S., Rittenhouse, S. E., Zvelebil, M. J., Stein, R. C., and Waterfield, M. D. (1997) *Biochem. J.* **326**, 139–147
- Brown, R. A., Domin, J., Arcaro, A., Waterfield, M. D., and Shepherd, P. R. (1999) *J. Biol. Chem.* **274**, 14529–14532
- Soos, M. A., Jensen, J., Brown, R. A., O'Rahilly, S., Shepherd, P. R., and Whitehead, J. P. (2001) *Arch. Biochem. Biophys.* **396**, 244–248
- Arcaro, A., Volinia, S., Zvelebil, M. J., Stein, R., Watton, S. J., Layton, M. J., Gout, I., Ahmadi, K., Downward, J., and Waterfield, M. D. (1998) *J. Biol. Chem.* **273**, 33082–33090
- Maffucci, T., Cooke, F. T., Foster, F. M., Traer, C. J., Fry, M. J., and Falasca, M. (2005) *J. Cell Biol.* **169**, 789–799
- Turner, S. J., Domin, J., Waterfield, M. D., Ward, S. G., and Westwick, J. (1998) *J. Biol. Chem.* **273**, 25987–25995
- Zhang, J., Banfic, H., Straforini, F., Tosi, L., Volinia, S., and Rittenhouse, S. E. (1998) *J. Biol. Chem.* **273**, 14081–14084
- Gaidarov, I., Smith, M. E., Domin, J., and Keen, J. H. (2001) *Mol. Cell* **7**, 443–449
- Brown, R. A., and Shepherd, P. R. (2001) *Biochem. Soc. Trans.* **29**, 535–537
- Ktori, C., Shepherd, P. R., and O'Rourke, L. (2003) *Biochem. Biophys. Res. Commun.* **306**, 139–143
- Katso, R. M., Pardo, O. E., Palamidessi, A., Franz, C., Marinov, M., De Laurentis, A., Downward, J., Scita, G., Ridley, A. J., Waterfield, M. D., and Arcaro, A. (2006) *Mol. Biol. Cell* **17**, 3729–3744
- Gaidarov, I., Zhao, Y., and Keen, J. H. (2005) *J. Biol. Chem.* **280**, 40766–40772

21. Meunier, F. A., Osborne, S. L., Hammond, G. R., Cooke, F. T., Parker, P. J., Domin, J., and Schiavo, G. (2005) *Mol. Biol. Cell* **16**, 4841–4851
22. Wang, Y., Yoshioka, K., Azam, M. A., Takuwa, N., Sakurada, S., Kayaba, Y., Sugimoto, N., Inoki, I., Kimura, T., Kuwaki, T., and Takuwa, Y. (2006) *Biochem. J.* **394**, 581–592
23. Bryant, N. J., Govers, R., and James, D. E. (2002) *Nat. Rev. Mol. Cell Biol.* **3**, 267–277
24. James, D. E. (2005) *J. Clin. Investig.* **115**, 219–221
25. Shepherd, P. R., Withers, D. J., and Siddle, K. (1998) *Biochem. J.* **333**, 471–490
26. Saltiel, A. R., and Pessin, J. E. (2003) *Traffic* **4**, 711–716
27. Kohn, A. D., Summers, S. A., Birnbaum, M. J., and Roth, R. A. (1996) *J. Biol. Chem.* **271**, 31372–31378
28. Cong, L. N., Chen, H., Li, Y., Zhou, L., McGibbon, M. A., Taylor, S. I., and Quon, M. J. (1997) *Mol. Endocrinol.* **11**, 1881–1890
29. Wang, Q., Somwar, R., Bilan, P. J., Liu, Z., Jin, J., Woodgett, J. R., and Klip, A. (1999) *Mol. Cell. Biol.* **19**, 4008–4018
30. Foran, P. G., Fletcher, L. M., Oatey, P. B., Mohammed, N., Dolly, J. O., and Tavare, J. M. (1999) *J. Biol. Chem.* **274**, 28087–28095
31. Kane, S., Sano, H., Liu, S. C., Asara, J. M., Lane, W. S., Garner, C. C., and Lienhard, G. E. (2002) *J. Biol. Chem.* **277**, 22115–22118
32. Berwick, D. C., Dell, G. C., Welsh, G. I., Heesom, K. J., Hers, I., Fletcher, L. M., Cooke, F. T., and Tavare, J. M. (2004) *J. Cell Sci.* **117**, 5985–5993
33. Gonzalez, E., and McGraw, T. E. (2006) *Mol. Biol. Cell* **17**, 4484–4493
34. Chang, L., Adams, R. D., and Saltiel, A. R. (2002) *Proc. Natl. Acad. Sci. U. S. A.* **99**, 12835–12840
35. Chiang, S. H., Hwang, J., Legendre, M., Zhang, M., Kimura, A., and Saltiel, A. R. (2003) *EMBO J.* **22**, 2679–2691
36. Kanzaki, M., Mora, S., Hwang, J. B., Saltiel, A. R., and Pessin, J. E. (2004) *J. Cell Biol.* **164**, 279–290
37. Inoue, M., Chiang, S. H., Chang, L., Chen, X. W., and Saltiel, A. R. (2006) *Mol. Biol. Cell* **17**, 2303–2311
38. Maffucci, T., Brancaccio, A., Piccolo, E., Stein, R. C., and Falasca, M. (2003) *EMBO J.* **22**, 4178–4189
39. Chaussade, C., Pirola, L., Bonnafous, S., Blondeau, F., Brenz-Verca, S., Tronchere, H., Portis, F., Rusconi, S., Payrastre, B., Laporte, J., and Van Obberghen, E. (2003) *Mol. Endocrinol.* **17**, 2448–2460
40. Ishiki, M., Randhawa, V. K., Poon, V., Jebailey, L., and Klip, A. (2005) *J. Biol. Chem.* **280**, 28792–28802
41. Kanda, H., Tamori, Y., Shinoda, H., Yoshikawa, M., Sakaue, M., Udagawa, J., Otani, H., Tashiro, F., Miyazaki, J., and Kasuga, M. (2005) *J. Clin. Investig.* **115**, 291–301
42. Kong, A. M., Horan, K. A., Sriratanana, A., Bailey, C. G., Collyer, L. J., Nandurkar, H. H., Shisheva, A., Layton, M. J., Rasko, J. E., Rowe, T., and Mitchell, C. A. (2006) *Mol. Cell. Biol.* **26**, 6065–6081
43. Govers, R., Coster, A. C., and James, D. E. (2004) *Mol. Cell. Biol.* **24**, 6456–6466
44. Li, C. H., Bai, L., Li, D. D., Xia, S., and Xu, T. (2004) *Cell Res.* **14**, 480–486
45. van den Hoff, M. J., Moorman, A. F., and Lamers, W. H. (1992) *Nucleic Acids Res.* **20**, 2902
46. Moyers, J. S., Bilan, P. J., Reynet, C., and Kahn, C. R. (1996) *J. Biol. Chem.* **271**, 23111–23116
47. Gillooly, D. J., Morrow, I. C., Lindsay, M., Gould, R., Bryant, N. J., Gaullier, J. M., Parton, R. G., and Stenmark, H. (2000) *EMBO J.* **19**, 4577–4588
48. Domin, J., Gaidarov, I., Smith, M. E., Keen, J. H., and Waterfield, M. D. (2000) *J. Biol. Chem.* **275**, 11943–11950
49. Didichenko, S. A., and Thelen, M. (2001) *J. Biol. Chem.* **276**, 48135–48142
50. Maffucci, T., Razzini, G., Ingrosso, A., Chen, H., Iacobelli, S., Sciacchitano, S., Quon, M. J., and Falasca, M. (2003) *Mol. Endocrinol.* **17**, 1568–1579
51. Niu, W., Huang, C., Nawaz, Z., Levy, M., Somwar, R., Li, D., Bilan, P. J., and Klip, A. (2003) *J. Biol. Chem.* **278**, 17953–17962
52. Ellson, C. D., Anderson, K. E., Morgan, G., Chilvers, E. R., Lipp, P., Stephens, L. R., and Hawkins, P. T. (2001) *Curr. Biol.* **11**, 1631–1635
53. Vieira, O. V., Botelho, R. J., Rameh, L., Brachmann, S. M., Matsuo, T., Davidson, H. W., Schreiber, A., Backer, J. M., Cantley, L. C., and Grinstein, S. (2001) *J. Cell Biol.* **55**, 19–25
54. Falasca, M., and Maffucci, T. (2006) *Arch. Physiol. Biochem.* **112**, 274–284
55. Arcaro, A., Khanzada, U. K., Vanhaesebroeck, B., Tetley, T. D., Waterfield, M. D., and Seckl, M. J. (2002) *EMBO J.* **21**, 5097–5108
56. Sindic, A., Aleksandrova, A., Fields, A. P., Volinia, S., and Banfic, H. (2001) *J. Biol. Chem.* **276**, 17754–17761
57. Visnjic, D., Crljen, V., Curic, J., Batinic, D., Volinia, S., and Banfic, H. (2002) *FEBS Lett.* **529**, 268–274
58. Jebailey, L., Rudich, A., Huang, X., Di Ciano-Oliveira, C., Kapus, A., and Klip, A. (2004) *Mol. Endocrinol.* **18**, 359–372
59. Mitra, P., Zheng, X., and Czech, M. P. (2004) *J. Biol. Chem.* **279**, 37431–37435
60. Chang, L., Chiang, S. H., and Saltiel, A. R. (2007) *Endocrinology* **148**, 27–33
61. Isakoff, S. J., Taha, C., Rose, E., Marcusohn, J., Klip, A., and Skolnik, E. Y. (1995) *Proc. Natl. Acad. Sci. U. S. A.* **92**, 10247–10251
62. Jiang, T., Sweeney, G., Rudolf, M. T., Klip, A., Traynor-Kaplan, A., and Tsien, R. Y. (1998) *J. Biol. Chem.* **273**, 11017–11024
63. Czech, M. P., and Corvera, S. (1999) *J. Biol. Chem.* **274**, 1865–1868
64. Jiang, Z. Y., Zhou, Q. L., Coleman, K. A., Chouinard, M., Boese, Q., and Czech, M. P. (2003) *Proc. Natl. Acad. Sci. U. S. A.* **100**, 7569–7574
65. van Dam, E. M., Gover, R., and James, D. E. (2005) *Mol. Endocrinol.* **19**, 1067–1077
66. Koumanov, F., Jin, B., Yang, J., and Holman, G. D. (2005) *Cell Metab.* **2**, 179–189
67. Bose, A., Robida, S., Furcinitti, P. S., Chawla, A., Fogarty, K., Corvera, S., and Czech, M. P. (2004) *Mol. Cell. Biol.* **24**, 5447–5458
68. Semiz, S., Park, J. G., Nicoloso, S. M., Furcinitti, P., Zhang, C., Chawla, A., Leszyk, J., and Czech, M. P. (2003) *EMBO J.* **22**, 2387–2399
69. Bose, A., Guilherme, A., Robida, S. I., Nicoloso, S. M., Zhou, Q. L., Jiang, Z. Y., Pomerleau, D. P., and Czech, M. P. (2002) *Nature* **420**, 821–824
70. Hodgkinson, C. P., Mander, A., and Sale, G. J. (2005) *Diabetologia* **48**, 1627–1636
71. Kawase, K., Nakamura, T., Takaya, A., Aoki, K., Namikawa, K., Kiyama, H., Inagaki, S., Takemoto, H., Saltiel, A. R., and Matsuda, M. (2006) *Dev. Cell* **11**, 411–421